RESEARCH ARTICLE
SOLID EARTH: GEOMAGNETISM

Earth and Planetary Physics
7: 39–48, 2023
doi: 10.26464/epp2023016

The study of geomagnetic jerk from 2010 to 2021 based on hourly mean data from global geomagnetic observatories

YiJun Li[1,2], Yan Feng[1,2,3*], SuQin Zhang[4], Shuang Liu[1,2], JinYuan Zhang[1], and GuanChun Wei[1]

[1]Institute of Space Weather, Nanjing University of Information Science & Technology, Nanjing 210044, China;

[2]State Key Laboratory of Lunar and Planetary Sciences, Macau University of Science and Technology, Macao 999078, China;

[3]State Key Laboratory of Space Weather, Chinese Academy of Sciences, Beijing 100190, China;

[4]Institute of Geophysics, China Earthquake Administration, Beijing 100081, China

Key Points:

- The secular variation in the global geomagnetic field in the most recent 10 years was analyzed.
- The covariance matrix method was adopted to remove the noise in the external field and was found to be a good replacement for the *Dst* and Ring Current (RC) indices.
- A new geomagnetic jerk was observed around 2018.0 and its characteristics were analyzed.

Citation: Li, Y. J., Feng, Y., Zhang, S. Q., Liu, S., Zhang, J. Y., and Wei, G. C. (2023). The study of geomagnetic jerk from 2010 to 2021 based on hourly mean data from global geomagnetic observatories. *Earth Planet. Phys.*, *7*(1), 39–48. http://doi.org/10.26464/epp2023016

Abstract: The secular variation in the global geomagnetic field was analyzed in terms of the annual differences in monthly means by using the hourly mean data from 18 foreign (outside China) observatories of the World Data Center (WDC) for Geomagnetism from January 2010 to January 2020 as well as 9 observatories in the Geomagnetic Network of China from January 2015 to April 2021. In addition, according to the correlation of noisy components from the observatories, a covariance matrix was constructed based on residuals between observations and the CHAOS-7.4 model to remove external contamination. Through a comparison before and after denoising, we found that the overall average standard deviations were reduced by 29.97% in China and by 41.4% outside China. Results showed the correlation coefficient between external noise (mainly the magnetosphere ring current) and the *Dst* index was 0.82, and the correlation coefficient between external noise and the Ring Current (RC) index reached 0.94. A geomagnetic jerk was globally discovered around 2018.0 on the geomagnetic eastward component *Y*. The jerk timing in China was around 2020.0, and the earliest one was in 2018.75, whereas the timing outside China was around 2018.0, and the earliest one was in 2017.67. This 2-year lag may have been caused by the higher electrical conductivity of the deep mantle. After more data were added, this jerk event was found to occur in an orderly manner in the northern hemisphere as the longitude increased and the intensity gradually increased as well. The variations in location of the jerk center were analyzed according to the CHAOS-7.4 model. Results revealed six extreme points distributed nearby the equator. The strongest was near the equator, at 170°E, and the strength gradually decreased as it extended to the northern and southern hemispheres. Another extreme point with the opposite sign was located at the equator, at 20°W, in the south-central part of the Atlantic, and the strength gradually decreased as it extended into Europe. The covariance matrix method can be used to analyze data from the Macau Science Satellite-1 mission in the future, and this method is expected to play a positive role in modeling and separating the large-scale external field.

Keywords: geomagnetic field; secular variation; jerk; covariance matrix

1. Introduction

The variation in the geomagnetic field with time covers different timescales. Malin et al. (1983) believed that short timescale changes are caused by currents in the ionosphere and magnetosphere and are related to solar activities (e.g., solar flares and coronal mass ejections), whereas long timescale changes were thought to be associated with activities in the Earth's interior (Alexandrescu et al., 1995, 1996; Le Huy et al., 1998; Bloxham et al., 2002). Investigating the secular variation (SV) of the geomagnetic field can provide a better understanding of the possible reasons for the formation of the geomagnetic field and the geophysical processes inside the Earth.

Geomagnetic jerk is considered a phenomenon of the shortest periodic change in the geomagnetic field caused by internal activities of the geomagnetic field. Courtillot et al. (1978) analyzed the annual mean values from geomagnetic observatories and found the first recorded geomagnetic jerk phenomenon in 1969. A magnetic jerk is defined as a sharp change in slope of the first derivative curve with respect to time; the curve presents

Correspondence to: Y. Feng, frank_feng8848@163.com
Received 24 OCT 2022; Accepted 07 NOV 2022.
Accepted article online 13 DEC 2022.

a∨or∧shape, which is particularly obvious in the eastward component *Y*. Since then, global jerk events in 1969, 1978, and 1991 and local jerk events in 1932, 1949, 1985, and 2003 have continued to be revealed (Alexandrescu et al., 1995, 1996; De Michelis et al., 1998; De Michelis and Tozzi, 2005; Olsen and Mandea, 2007). Olsen and Mandea (2008) advanced the theory that a global geomagnetic jerk may be the result of the superposition of local geomagnetic jerks that occur at different times. In addition, results by Pinheiro and Jackson (2008) implied that the time delay of a jerk might be caused by the propagation of a single event in the mantle. In the past several decades, researchers have adopted a variety of methods to study the characteristics of jerk, such as wavelet analysis (Alexandrescu et al., 1996) and nonlinear chaotic analysis (Qamili et al., 2013), to inspect the time of jerk, strength of jerk, and so on. Torta et al. (2015) and Feng Y et al. (2018) analyzed the jerk events in 2014 and 2003.5 and calculated the jerk time and strength by using data from geomagnetic observatories. In recent years, the frequency of jerk has become higher; consequently, the study of each jerk has become more detailed. The critical step in precisely determining a jerk, however, is to remove the external contamination in an appropriate way.

The external field noise generated by the currents in the Earth's ionosphere and magnetosphere overlaps the change period of the internal field, especially the induced magnetic field generated by this noise, which cannot be completely separated from the internal field. This is the main contamination to consider when studying the SV of the internal field. As a result, the remodeled external signals have to be approximated and removed. Gubbins and Tomlinson (1986) studied jerk by using the *Kp* index as the criterion for the monthly mean value of the quiet time. To eliminate the noise of the external field from the original data series obtained through satellites and geomagnetic observatories, they deleted data for the period when the external magnetic field activity was high. Their results showed that the monthly mean values could be used to provide low-noise and high-temporal-resolution records. The average value based on the midnight value of the International Day of Quiet was less disturbed by external magnetic fields than was the average value of all the days.

To study jerk, scientists have completed extensive work to obtain clean SV data by removing the noise signal from external sources in different ways. De Michelis and Tozzi (2005) proposed a method to remove external noise from the annual mean values through the use of the *Dst* index. They used *Dst* data in the selected period to correct the observatory data, largely expanding the range of available data compared with the method of Gubbins and Tomlinson (1986), although it was valid only for the eastward component *Y*. Verbanac et al. (2009) proposed an improved method that combined the International Geomagnetic Reference Field global geomagnetic field model and the *Dst* index to correct the noise from the annual mean value of the observatory. Olsen and Mandea (2008) attempted to parameterize external field sources as part of the field model and apply model correction to the observation data. To eliminate the noise and analyze the SV trend of the main field, they used indices such as the *Dst* or *Kp* to parameterize the noisy component of the external field when constructing the global model. However, this method did not consider the possible conductive structure of the local mantle and the differences in mantle conductivity; consequently, the time of occurrence and the intensity of the induced field would be different. Moreover, the global model constructed by this method forced researchers to ignore many local anomalies when the local SV were analyzed.

Recently, Wardinski and Holme (2011) proposed a method in which they constructed a covariance matrix by using the residuals between the model and the observations to remove the remodeled external SV signal. They illustrated that the residual could ideally replace the *Dst* index in the calculation as a proxy for the remodeled external signals, which could be seen as the large-scale magnetosphere ring current. Removing these external signals largely reduced the standard deviation of the data, thereby improving the resolution of internal features (such as jerk). Compared with the method of Gubbins and Tomlinson (1986), which used the *Kp* index to filter the suitable time series, the method proposed by Wardinski and Holme (2011) greatly expanded the range of available time series and improved the continuity of data, but the latter significantly depends on the geomagnetic index (i.e., *Dst*, *Kp*) to correct it. In this study, we made further improvements by adopting the method of constructing a covariance matrix, but we selected the noisy components from different observatories to remove the external source field noise. This method no longer relied on the geomagnetic index in the process of denoising.

2. Data and Methods

2.1 Data

Most of the data used in this study came from the World Data Center (WDC) for Geomagnetism in Edinburgh, from which we selected 18 foreign (outside China) geomagnetic observatories from January 2010 to January 2020. These geomagnetic observatories had features such as even spatial coverage, particularly in Europe, continuous data recording, and accurate hourly mean data with high precision. To analyze the SV of the geomagnetic field over China, 9 Chinese geomagnetic observatories from January 2015 to April 2021 were uniformly selected from the Geomagnetic Network of China, Chinese Earthquake Administration (the records of some observatories were missing from 2010 to 2015). The geographic locations of all 27 observatories are shown in Figure 1.

Because we mainly focused on the SV of the internal field, the monthly mean values of the three components (northward *X*, eastward *Y*, and vertically downward *Z*) from each observatory were calculated based on the obtained hourly mean value, thereby eliminating high-frequency external noise. According to the general process, we simply determined the annual differences in the monthly means as the SV to analyze the possible jerk of the geomagnetic field. This method largely reduced the influence of the annual periodic changes in the geomagnetic field. The specific calculation method can be written as

$$\frac{\mathrm{d}B}{\mathrm{d}t} = B_{t+6} - B_{t-6}, \tag{1}$$

where *B* is the geomagnetic component *X*, *Y*, or *Z*, and *t* is the

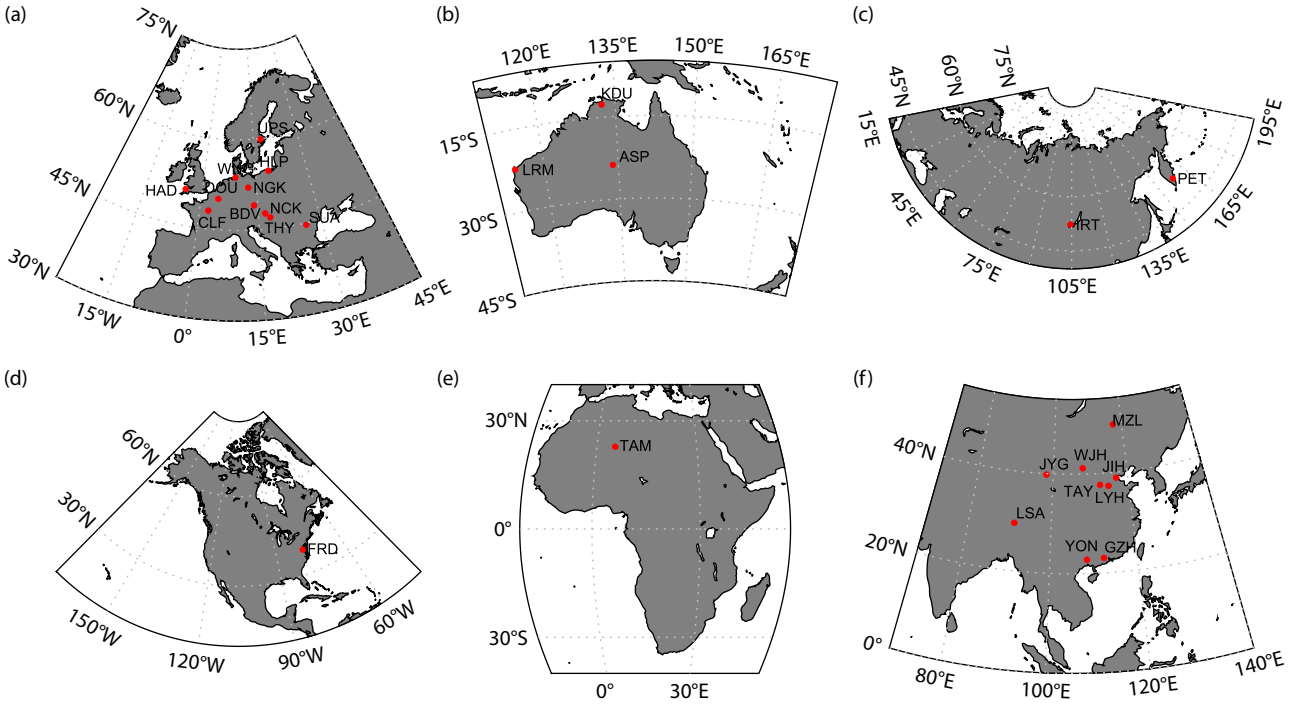

Figure 1. Distribution of all 27 geomagnetic observatories. (a) Observatories in Europe; (b) observatories in Australia; (c) observatories in Asia; (d) observatories in North America; (e) observatories in Africa; (f) observatories in China. Albers projection. (Abbreviations in the figure represent observatory names.)

month.

2.2 Methods

Wardinski and Holme (2011) proposed a method to remove the noise signal from the magnetosphere ring current that could effectively reduce the standard deviation of the data and improve the resolution of the geomagnetic jerk feature. The information on the noise signal is contained in the SV residual between the observation data and the simulated value of the geomagnetic field model. The coherent signal between the SV residuals in the *X*, *Y*, and *Z* components of each observatory can be described by a 3 × 3 covariance matrix:

$$\mathrm{cov}(p,q)=\frac{\sum_{i=1}^{n}P_iQ_i}{n}, \tag{2}$$

where *P* and *Q* are SV residual between the observation data and the simulated value of the geomagnetic field model from each observatory, *p* and *q* are vectors of SV residual, and *n* is the length of the vector. We considered the correlation of data residuals within each observatory. The covariance matrix was block diagonal with 3 × 3 blocks and could be inverted easily. The eigenvalues of a real symmetric matrix are real and its eigenvectors are orthogonal; the eigenvectors and the eigenvalues are known. According to the direction corresponding to the eigenvalues from small to large, direction 1 was the least disturbed ("quiet"), direction 2 was more disturbed ("medium"), and direction 3 was most disturbed ("noisy"). The contribution of the noisy component was highly correlated with the *Dst* and Ring Current (RC) indices. Because the contribution of the noisy component is mainly caused by external field activities, this component of the calibration observatory can replace the *Dst* index, and the zero-lag correlation function can be used to remove the coherent signals between the residual noisy components from different observatories. Therefore, a cleaner SV series with reduced external contamination can be obtained without depending on the geomagnetic indices. The Niemegk (NGK) Geomagnetic Observatory in Germany has complete data series from 2010 to 2019 with high precision and reliability. We used the NGK SV records and the residuals between the CHAO-7.4 model simulations to correct the external signals of the observatories (except China) according to the following formula:

$$\dot{r}_{\mathrm{corrected}}(t_k)=\dot{r}_{\mathrm{noisy}}(t_k)-\frac{\sum_l\dot{C}(t_l)\,\dot{r}_{\mathrm{noisy}}(t_l)}{\sum_l\dot{C}(t_l)^2}\dot{C}(t_k), \tag{3}$$

where $\dot{r}_{\mathrm{corrected}}$ is the noisy component of the corrected SV residual, $\dot{r}_{\mathrm{noisy}}$ is the noisy component of the uncorrected SV residual, $\dot{C}$ is the annual variation in the *Dst* index or the noisy component of the uncorrected SV residual of the selected component, and subscripts *k* and *l* are the numbers of time samples. This correction method is applicable to only the noisy component. The corrected noisy component is then combined with the uncorrected clean and general components and converted back to the original components *X*, *Y*, and *Z*. Therefore, this process removes the external signal from the residual of the noisy component, and when rotated back to geographic coordinates, the signal is removed from each component based on the correlation strength of the external signal.

In addition, in this study we chose the newest version of the CHAOS-7 (Finlay et al., 2020) geomagnetic model, CHAOS-7.4, to construct the covariance matrix. This model was created by the magnetic field observation data collected by the low-Earth-orbiting satellites Swarm, CryoSat-2, CHAMP, SAC-C, and Oersted, and

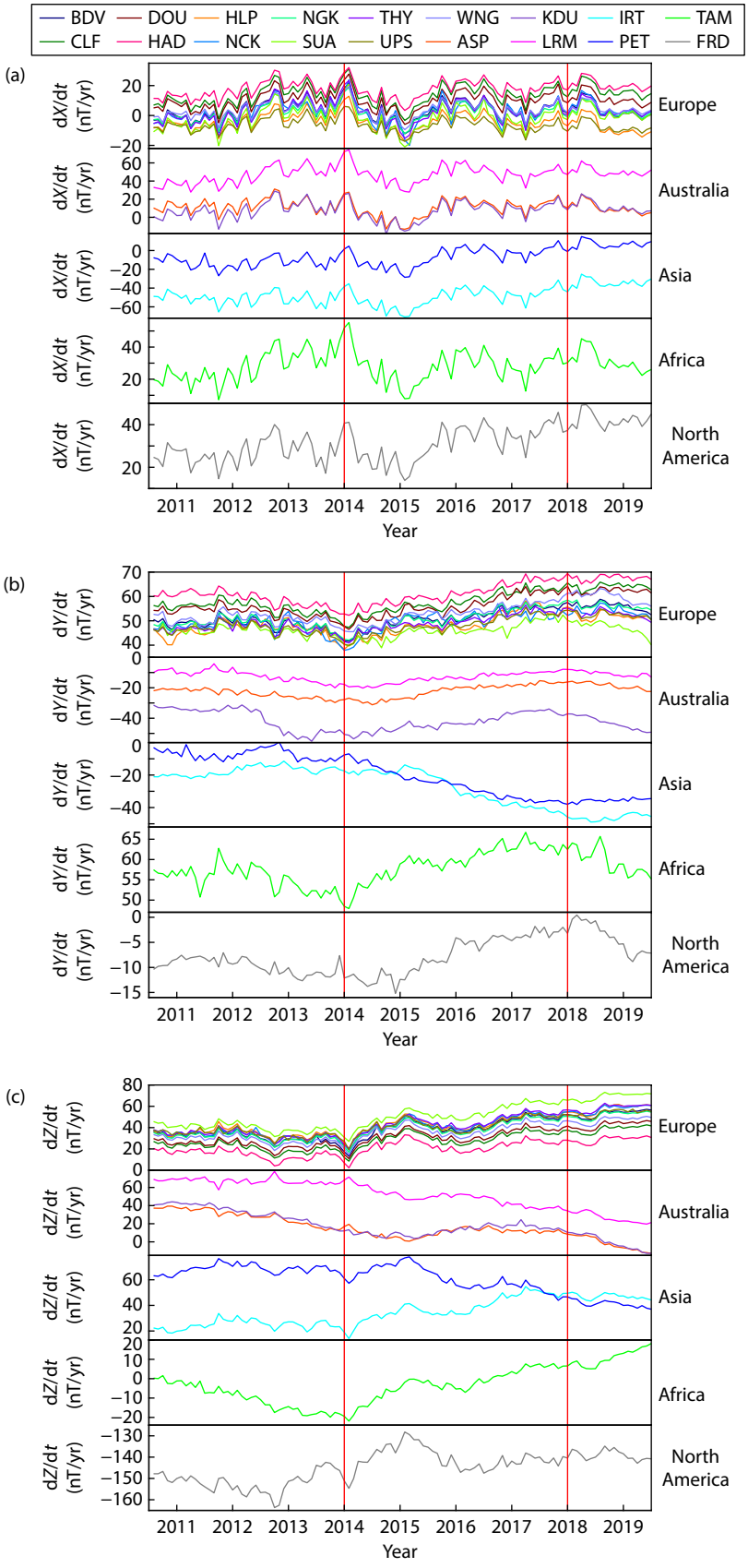

Figure 2. The secular variation (SV) in components *X*, *Y*, and *Z* from 18 foreign observatories with undenoised data. (a) Component *X*; (b) component *Y*; (c) component *Z*. Red lines: 2014.0 and 2018.0. (Abbreviations in the legend represent observatory names.)

the annual difference in the monthly mean value of the observatory. The temporal span of the model was from 1999 to 2020. The model was able to provide a state-of-the-art simulation of the geomagnetic SV.

3. Results

The SV of components *X*, *Y*, and *Z* from all 27 observatories without the external contamination removed are listed in Figure 2, and those from all 9 observatories in China without the external contamination removed are listed in Figure 3.

Figure 2 shows good agreement in the SV among European observatories. For *X*, there is good consistency among the five continents. The same is true for *Y* and *Z* except for the continents of Asia and Australia. Figure 3 shows the SV in a different time span, but the trends are basically the same. Figure 2b clearly illustrates that the obvious jerk shape occurs at BDV, CLF, DOU, HAD, HLP, NCK, NGK, SUA, THY, UPS, WNG, ASP, KDU, LRM, TAM, and FRD observatories and is consistent with the results of Torta et al. (2015). The jerk recorded by KDU occurred earlier, around 2013.42, and the jerk from FRD observatory occurred later, around 2014.92; however, there were no clear geomagnetic jerk signals in the 9 Chinese observatories. A new jerk event was found in the *Y* component for all 27 observatories, as shown in Figures 2b and 3. In terms of the occurrence time, the observatories outside China recorded jerk events basically around 2018.0, and among them, the event recorded by the KDU observatory occurred earlier. All Chinese observatories showed this jerk somewhat later and then an occurrence around 2020.

It was difficult to determine the jerk shape in components *X* and *Z* in both the Chinese and foreign SV trends. An interesting finding was the high consistency in the SV trend between observatories far away from each other. A possible reason is that the undenoised data contained strong external field noises that are mainly generated by the current in the Earth's magnetosphere, which concealed the SV trend of the internal field. It was necessary to denoise the data before further analyzing the characteristics of the new geomagnetic jerk.

Here, we used the monthly mean data from the observatories to construct the covariance matrix to obtain the noisy component and to explore the correlation between the noisy component and the geomagnetic index according to Equation (4):

$$r = \frac{\sum_{i=1}^{n}(x_i - \bar{x})(y_i - \bar{y})}{\sqrt{\sum_{i=1}^{n}(x_i - \bar{x})^2}\sqrt{\sum_{i=1}^{n}(y_i - \bar{y})^2}}, \tag{4}$$

where x is the annual variation in the *Dst* index or the RC index, $\bar{x}$ is the average annual variation in the *Dst* index or RC index, y is the annual difference in the noisy component of the uncorrected SV residual, and $\bar{y}$ is the average annual variation in the noisy component of the uncorrected SV residual.

As shown in Figure 4, we compared the average value of the noise contribution from 18 foreign observatories from 2010.5 to 2015.0 with the annual differences in monthly means of the *Dst* index from Equation (4). The correlation coefficient was 0.82. Because the final *Dst* index obtained from the WDC observatory had been updated only to the end of 2014.0, the annual difference in the RC index was calculated from the CHAOS-7.4 model to compare with the average value of the noisy components from the 18 regional observatories, as shown in Figure 5. The correlation reached 0.94. These two correlation values confirmed that the noise from each observatory actually contained the current caused by the magnetosphere ring current. There was a strong correlation of the noisy components between the different observatories (Table 1).

Table 1 provides the exact correlation values between 17 observatories and the NGK. The CLF observatory is geographically close to the NGK, which resulted in the highest correlation, 0.99. In contrast, the ASP, KDU, and LRM observatories are far away from the NGK, so the correlation was relatively low, 0.60, 0.66, and 0.63, respectively. For comparison purposes, the NGK observatory was set as the standard observatory. Its noisy component was used to replace the *Dst* index, and the zero-lag correlation function was adopted to denoise the data so that the entire process of denoising

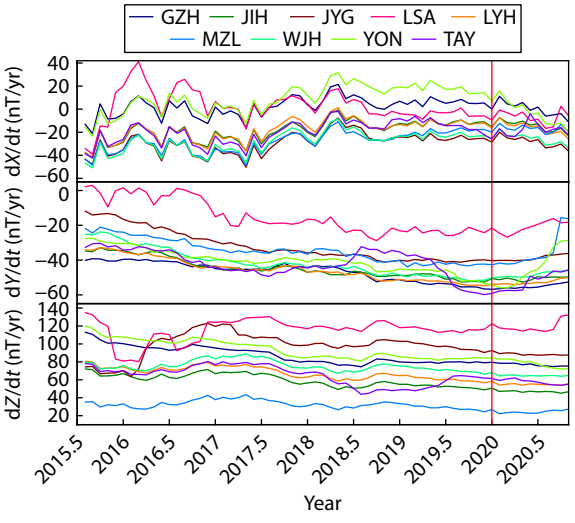

Figure 3. The secular variation in components *X*, *Y*, and *Z* from 9 Chinese observatories with undenoised data. Red line: 2020.0.

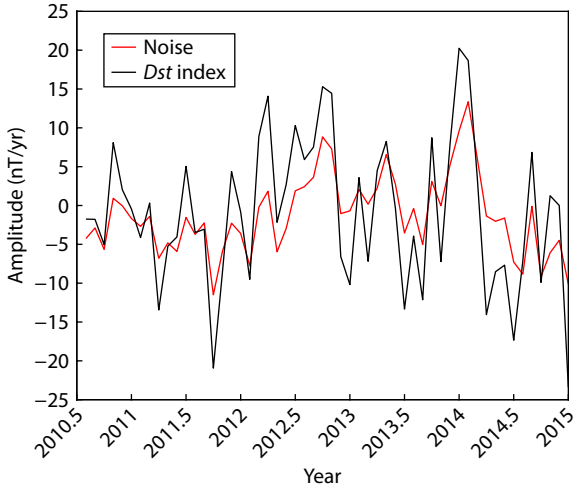

Figure 4. Comparison of the average noise contribution of the 18 foreign observatories and the annual difference in monthly means of the *Dst* index.

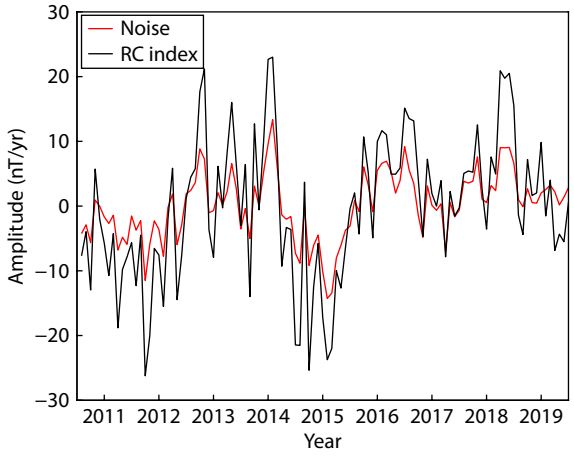

Figure 5. Comparison of the average noise contribution from 18 foreign observatories, and the annual difference in the monthly means of the RC index.

Table 1. Correlation between 17 foreign observatories and the Niemegk (NGK) Geomagnetic Observatory in Germany.

Observatory	Longitude (°)	Latitude (°)	Correlation
BDV	14.02E	49.08N	0.98
CLF	2.26E	48.03N	0.99
DOU	4.60E	50.10N	0.99
HAD	4.48W	51.00N	0.99
HLP	18.82E	54.61N	0.97
NCK	16.72E	47.63N	0.98
SUA	26.25E	44.68N	0.99
THY	17.89E	46.90N	0.99
UPS	17.35E	59.90N	0.99
WNG	9.05E	53.73N	0.99
ASP	133.88E	23.76S	0.60
FRD	77.37W	38.21N	0.83
IRT	104.45E	52.27N	0.96
KDU	132.47E	12.69S	0.66
LRM	114.10E	22.22S	0.63
PET	158.25E	52.97N	0.94
TAM	5.53E	22.79N	0.91

did not depend on the geomagnetic index.

Here we approximate the *Dst* trend from Equation (3) to remove external noise. After the covariance matrix was used to remove external noise, the reliability of the data was significantly improved. We analyzed the average standard deviation between the observed values and CHAOS-7.4 in the *X*, *Y*, and *Z* components before and after denoising. The average standard deviations are listed in Table 2.

The deviation had the largest decrement in the *X* component, which decreased by 53.8%. This was followed by component *Z*, which decreased by 47.8%. Component *Y* had the smallest decrement of only 22.8%. The overall deviation was reduced by 41.5%.

Table 2. Average standard deviations between 18 foreign observatories and CHAOS-7.4 values before and after denoising.

Component	Before (nT/yr)	After (nT/yr)
X	7.16	3.31
Y	2.15	1.66
Z	4.48	2.34

Table 3. Average standard deviations between the 9 Chinese observatories and the CHAOS-7.4 values before and after denoising.

Component	Before (nT/yr)	After (nT/yr)
X	10.16	5.00
Y	3.45	3.23
Z	8.10	5.47

These results confirmed that the noise generated by the external field was mainly in the *X* and *Z* components and that the disturbance was minimal because component *Y* is parallel to the equatorial ring current.

The same method was used to denoise the data from the Chinese observatories. The residuals between the observation values of the LYH observatory and the model approximations were selected to remove the external noise. The results are shown in Table 3.

The results showed that the average standard deviation had the largest decrement in component *X* and that the deviation was reduced by 50.8%. Components *Z* and *Y* were reduced by 32.5% and 6.6%, and finally the overall deviation was reduced by 30.0%.

After creating the covariance matrix of residuals to eliminate the external noise, a set of relatively clean SV series was obtained, especially in component *Y*, which was minimally interfered with by the external field. The results are shown in Figures 6 and 7.

Figure 6 shows tiny differences compared with the SV without denoising, especially in components *X* and *Z*. Figure 6b reveals the obvious jerk events that occurred among the 18 foreign observatories in 2014.0 and 2018.0 in component *Y*. Among them, the European observatories have close geographical locations; consequently, they have consistent long-term trends and similar occurrence times. Large differences of distance and time were found between Australia and Europe. For example, the occurrence time of jerk at KDU observatory was the earliest. The SV trends of IRT and PET observatory in Asia were highly consistent, but the latter had no obvious sign of the 2014.0 jerk. Both the TAM observatory located in Africa and the FRD observatory located in North America showed obvious records of this jerk event. Regarding the 2018.0 jerk event, whose strength was strong in Europe, the SV in component *Y* can be seen around 2018.0, whereas the 9 observatories in China did not record any obvious geomagnetic jerk characteristics, as shown in Figure 7. However, jerk was captured around 2020.0, particularly in the MZL observatory. Two jerks could not be found in components *X* and *Z*, as shown in Figures 6 and 7. Components *X* and *Z* still contained the interference signal of the external source field. Therefore, we focused on the characteristics of the 2018.0 geomagnetic jerk in overseas regions and the 2020.0 geomagnetic jerk in the region of China in component *Y* for further study. To inspect the SV trend of component *Y* through

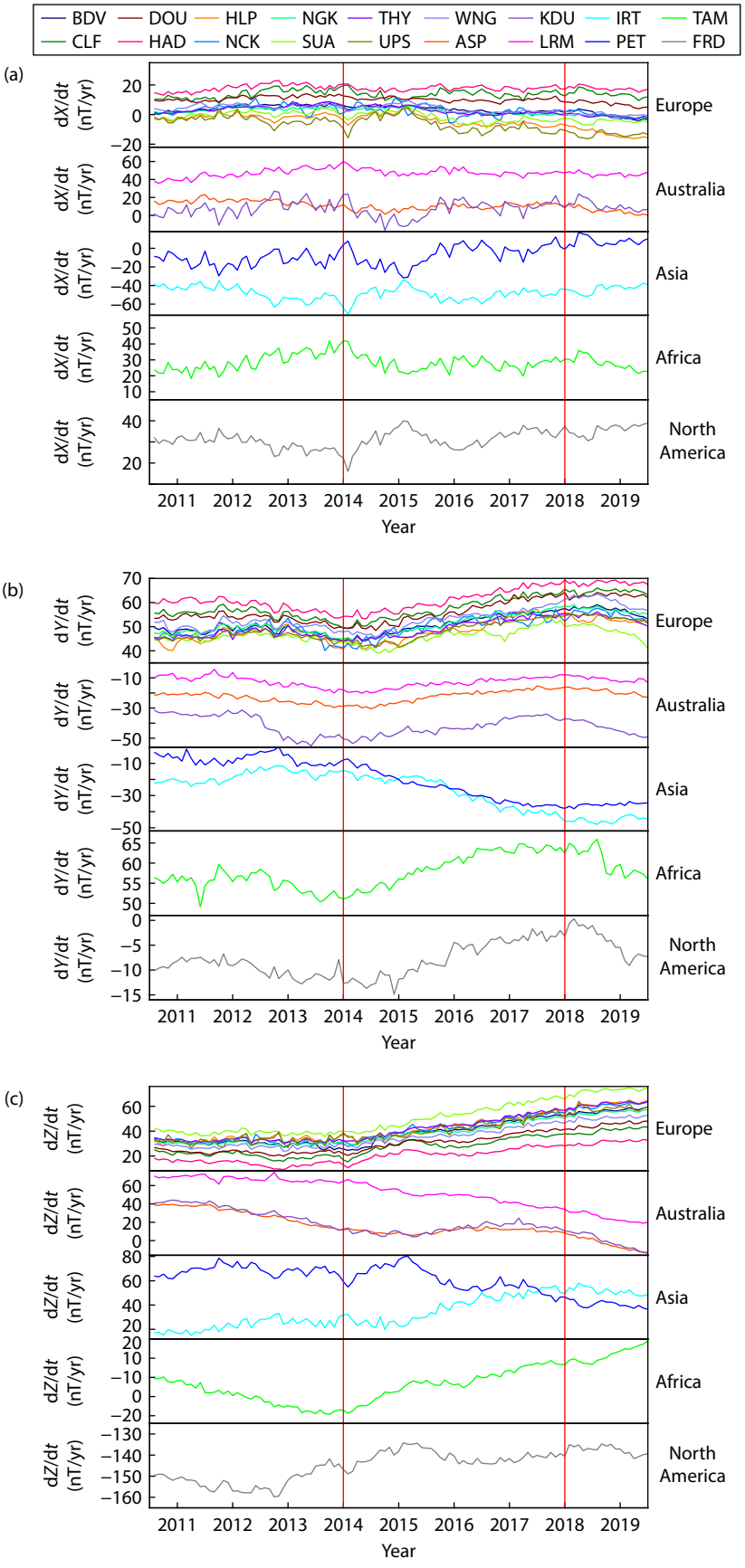

Figure 6. The secular variation of components *X*, *Y*, and *Z* from 18 foreign observatories with denoised data. (a) Component *X*; (b) component *Y*; (c) component *Z*. Red lines: 2014.0 and 2018.0.

the CHAOS-7.4 model, we took NGK observatory as example to linearly approximate the SV and found a good fit with the SV of the observed data after the denoising process, as shown in Figure 8.

To quantitatively describe the characteristics of jerk, we calculated the secular acceleration value of each observatory before and after jerk and the occurrence time. The secular acceleration value was directly calculated from the time series by piecewise linear fitting. The specific method was to visually check the SV of *Y* and the jerk event, fix the starting and end points of the time series, and then linearly fit the SV trend in the selected time period. The slope difference of the fitted straight line before and after jerk was defined as the jerk strength (Macmillan, 1996). By changing the crossing time of two adjacent fitted straight lines, we could obtain the final turning time on the basis of the best fitting effect obtained, which was the time the jerk occurred. The results are listed in Table 4 and 5.

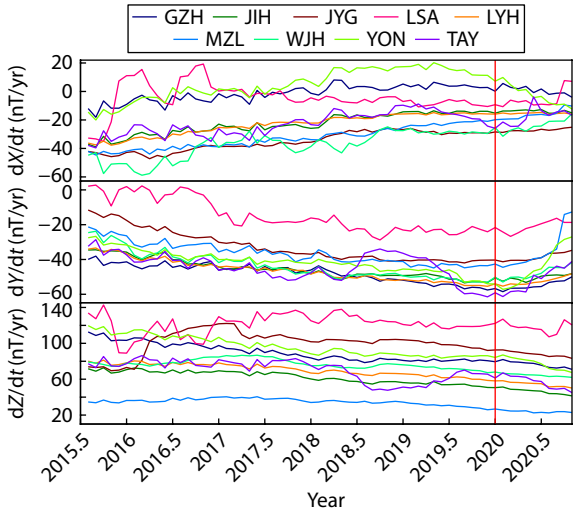

Figure 7. The secular variation of components *X*, *Y*, and *Z* from 9 Chinese observatories with denoised data. Red line: 2020.0.

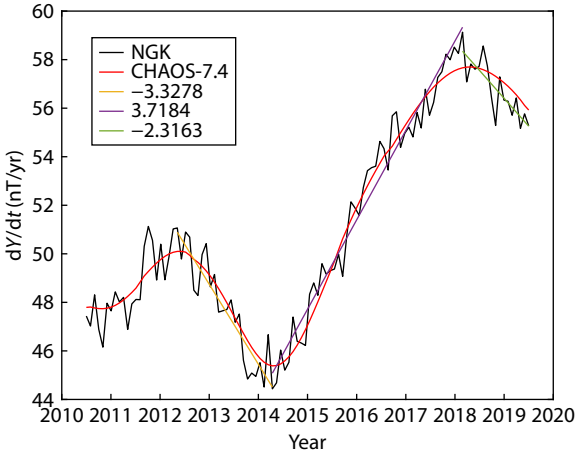

Figure 8. Comparison of the secular variation between the Niemegk (NGK) Observatory and the CHAOS-7.4 model. Black line: observation value; red line: simulation value; orange, purple, and green line segments: the best simulation based on the observation value after the jerk time was selected.

All 18 foreign observatories, except PET in Asia, recorded the time and strength of geomagnetic jerks in 2014.0 and 2018.0. For the 2014.0 event, that at KDU observatory in Australia occurred the earliest, in 2013.42, whereas that at SUA observatory in Europe occurred the latest, in 2014.67. Most observatories were concentrated around 2018.58. The absolute strength of the jerk at KDU observatory reached the maximum, at 11.64 nT/yr^2. For the 2018.0 event, that at KDU observatory occurred the earliest as well, in 2017.67, and that at the HAD observatory in Europe occurred the latest, in 2018.92. The absolute strength of the event at KDU reached the maximum, at −12.32 nT/yr^2. In the region of China, 9 observatories recorded the jerk event around 2020.0, as shown in Figure 5. Among them, that at LSA observatory occurred the earli-

Table 4. Time and strength of geomagnetic jerks at 18 foreign observatories.

Observatory	2014.0 jerk time (yr)	Strength (nT/yr^2)	2018.0 jerk time (yr)	Strength (nT/yr^2)
BDV	2014.17	6.69	2018.58	−8.98
CLF	2014.00	7.30	2018.58	−5.19
DOU	2014.58	5.70	2018.58	−5.03
HAD	2014.42	5.97	2018.92	−5.03
HLP	2014.33	10.40	2018.00	−6.02
NCK	2014.25	10.29	2018.58	−8.25
NGK	2014.33	7.05	2018.17	−6.03
SUA	2014.67	6.49	2017.92	−8.63
THY	2014.17	5.66	2018.58	−8.08
UPS	2014.58	6.50	2018.58	−6.32
WNG	2014.58	6.61	2018.58	−11.62
ASP	2014.50	6.68	2018.08	−7.75
FRD	2014.42	4.54	2018.17	−9.71
IRT	2014.00	−10.19	2018.58	12.20
KDU	2013.42	11.64	2017.67	−12.32
LRM	2014.33	6.53	2017.92	−5.94
PET	—	—	2018.17	6.51
TAM	2013.58	9.23	2018.17	−9.71

Table 5. Time and strength of geomagnetic jerks at 9 Chinese observatories.

Observatory	2020.0 jerk time (yr)	Strength (nT/yr^2)
GZH	2020.08	13.64
JIH	2019.67	9.52
JYG	2019.67	15.33
LSA	2018.75	11.89
LYH	2019.92	11.65
MZL	2019.67	13.84
WJH	2019.67	15.10
YON	2020.00	22.20
TAY	2019.92	16.60

est, in 2018.75, whereas that at GZH occurred the latest, in 2020.08. In terms of strength, that at the YON observatory reached the maximum, at 22.20 nT/yr^2.

To explain the aforementioned phenomena, we found that the timing of the jerk between SUA and LSA observatory was very close, and a timing gap of one year or longer occurred among the other observatories. To explore the possible reason for the jerk timing difference, through expansion of the available data, we selected 10 new geomagnetic observatory data from the WDC observatory, carried out the denoising process, and finally calculated the jerk time and strength. The jerk occurrence time and strength of the total 37 observatories are shown in Figures 9 and 10.

When the jerk occurrence time was considered, BDV, CLF, DOU, HAD, NCK, NGK, THY, UPS, WNG, FRD, IRT, PET, TAM, GZH, JIH, JYG, LSA, LYH, MZL, WJH, YON, TAY, BOU, FRN, and ABG observatories in North America, Europe, Africa, and Asia were generally later than 2018.08. Among them, the times in North America and Africa were closest to 2018.0, whereas the jerk time in China was the latest and those in Europe were between the times in North America and China. At the junction of Asia and Europe and throughout the entire southern hemisphere, the occurrence times were no later than 2018.0. The EYR observatory in New Zealand had the earliest occurrence time, in 2016.0. Times at the Asia–Europe border where it is close to Europe and in South America were quite close to 2018.0. On the whole, the occurrence times showed a sequential trend from North America to Europe and then to Asia in the northern hemisphere, except at the border of Asia and Europe.

Regarding the jerk strength, the EYR observatory in New Zealand reached the maximum intensity, at 23.57 nT/yr^2. In the northern hemisphere, from North America to Europe and then to Asia, the jerk intensity showed an increasing trend. All in all, there were obvious regular changes in the northern hemisphere but no obvious trend in the southern hemisphere.

Even when the data were expanded to include 37 observatories, most regions and oceans were still not covered. To explore the strength of various regions around the world, we used the CHAOS-7.4 model to draw a global strength map of the jerk, as shown in Figure 11.

As shown in Figure 11, six jerk strength centers are distributed near the equator, the most extreme of which is at the equator, at 170°E. It extends to the northern and southern hemispheres, and the strength gradually decreases with latitude. The other region at the equator, at 20°W, lies in the central and southern Atlantic and extends to Europe. It shows a closed intensity but with opposite signs, and its strength gradually decreases. The remaining strength centers exist in the central Pacific Ocean, eastern Pacific Ocean, northern Indian Ocean, and Indonesia. However, compared with the 2014.0 jerk, a western drift trend can be found in the eastern Pacific Ocean.

4. Conclusions

We analyzed the SV data from the WDC observatory from 2010.0 to 2020.0 and from the China Earthquake Administration's Geomagnetic Network Center from 2015.0 to 2021.4. The residuals between the SV of measured values and the CHAOS-7.4 model were used to construct a covariance matrix. The noisy component could then be approximated to replace the *Dst* index, and a function based on the zero-lag correlation was used to remove the coherent signal between the residual noisy components from different observatories and obtain a clean data series.

After inspecting and describing the preliminary results, we reached the following conclusions:

(1) The correlations between the average noisy component from 18 foreign observatories and the *Dst* and RC indices were 0.82 and 0.94, which imply that the noise contained obvious interference signals generated by the magnetosphere ring current. On the basis of the high correlations of noise between different observatories, we used the noise of specific observatories instead of the *Dst* index to achieve a better denoising effect, improve the quality of the data, and separate the denoising process from dependency on geomagnetic indices.

(2) A 2-year lag in the region of China about the 2018.0 jerk was recorded by other foreign observatories. This lag may have been caused by the higher electrical conductivity of the deep mantle, consistent with the suggestion by Pinheiro et al. (2011). Brown et al. (2016) showed that the relationships among the time delay of the jerk, the mantle conductivity, and other properties may not follow simple or constant rules. A better understanding of the cause of jerk is needed to explain the observed changes. The

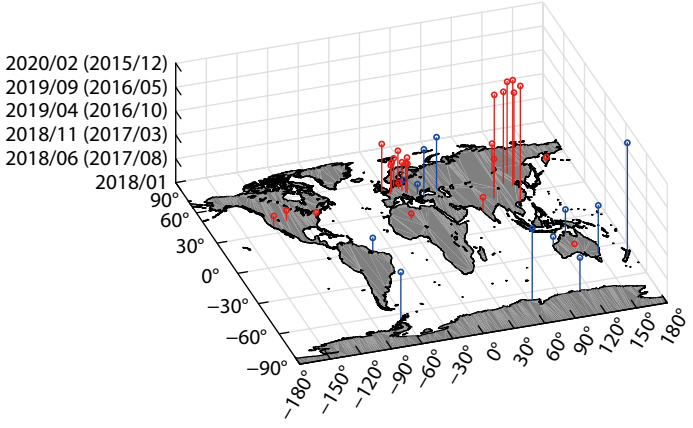

Figure 9. Jerk time from 37 observatories around the world. Zero altitude: 2018.0; blue lines: earlier than 2018.0; red lines: later than 2018.0.

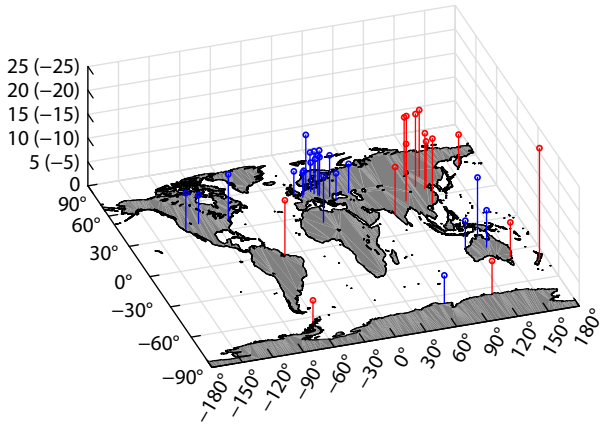

Figure 10. Jerk strength distribution from 37 observatories around the world. Zero height: strength is 0; blue lines: negative values; red line: positive values.

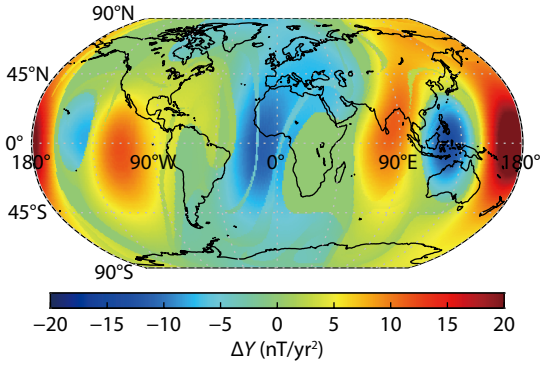

Figure 11. Global strength map of the jerk of component *Y* based on the CHAOS-7.4 model from 2017.0 to 2021.0.

coming Macau Science Satellite-1 with high-quality data may offer a good opportunity to determine the reason and investigate even further.

(3) According to the modeling by CHAOS-7.4, six strength centers are distributed around the equator, consistent with the results of Torta et al. (2015). We suggest there are several fixed geographic regions of jerk strength in the *Y* component, but there may be a slight left-to-right shift in the center region.

Acknowledgments

We acknowledge the support of the National Natural Science Foundation of China (Nos. 42030203, 41974073, 41404053, 42250103), the Macau Foundation and the pre-research project of Civil Aerospace Technologies (Nos. D020308 and D020303), which is funded by the China National Space Administration. We also acknowledge support from the opening fund of the State Key Laboratory of Lunar and Planetary Sciences (Macau University of Science and Technology, Macau Science and Technology Development Fund [FDCT] No. 119/2017/A3), the Specialized Research Fund for State Key Laboratories, and the NUIST-UoR International Research Institute. We thank the Geomagnetic Network of China, Institute of Geophysics, Chinese Earthquake Administration, for the data resources. We also thank the reviewers for their valuable advice.

References

Alexandrescu, M., Gibert, D., Hulot, G., Le Mouël, J. L., and Saracco, G. (1995). Detection of geomagnetic jerks using wavelet analysis. *J. Geophys. Res.: Solid Earth*, *100*(B7), 12557–12572. https://doi.org/10.1029/95jb00314

Alexandrescu, M., Gibert, D., Hulot, G., Le Mouël, J. L., and Saracco, G. (1996). Worldwide wavelet analysis of geomagnetic jerks. *J. Geophys. Res.: Solid Earth*, *101*(B10), 21975–21994. https://doi.org/10.1029/96JB01648

Bloxham, J., Zatman, S., and Dumberry, M. (2002). The origin of geomagnetic jerks. *Nature*, *420*(6911), 65–68. https://doi.org/10.1038/nature01134

Brown, W., Beggan, C., and Macmillan, S. (2016). Geomagnetic jerks in the Swarm era. *In: Spacebooks. ESA Living Planet Symposium*, *Czech*, *Prague*, 9–13.

Courtillot, V., Ducruix, J., and Le Mouël, J. L. (1978). Sur une accélération récente de la variation séculaire du champ magnétique terrestre. *C. R. Acad. Sci. Paris. Ser. D*, *287*, 1095–1098.

De Michelis, P., Cafarella, L., and Meloni, A. (1998). Worldwide character of the 1991 geomagnetic jerk. *Geophys. Res. Lett.*, *25*(3), 377–380. https://doi.org/10.1029/98gl00001

De Michelis, P., and Tozzi, R. (2005). A Local Intermittency Measure (LIM) approach to the detection of geomagnetic jerks. *Earth Planet. Sci. Lett.*, *235*(1–2), 261–272. https://doi.org/10.1016/j.epsl.2005.04.001

Feng, Y., Holme, R., Cox, G. A., and Jiang, Y. (2018). The geomagnetic jerk of 2003.5—Characterisation with regional observatory secular variation data. *Phys. Earth Planet. Inter.*, *278*, 47–58. https://doi.org/10.1016/j.pepi.2018.03.005

Finlay, C. C., Kloss, C., Olsen, N., Hammer, M. D., Tøfner-Clausen, L., Grayver, A., and Kuvshinov, A. (2020). The CHAOS-7 geomagnetic field model and observed changes in the South Atlantic Anomaly. *Earth Planets Space*, *72*, 156. https://doi.org/10.1186/s40623-020-01252-9

Gubbins, D., and Tomlinson, L. (1986). Secular variation from monthly means from Apia and Amberley magnetic observatories. *Geophys. J. Int.*, *86*(2), 603–616. https://doi.org/10.1111/j.1365-246x.1986.tb03846.x

Le Huy, M., Alexandrescu, M., Hulot, G., and Le Mouël, J. L. (1998). On the characteristics of successive geomagnetic jerks. *Earth Planets Space*, *50*(9), 723–732. https://doi.org/10.1186/BF03352165

Macmillan, S. (1996). A geomagnetic jerk for the early 1990's. *Earth Planet. Sci. Lett.*, *137*(1–4), 189–192. https://doi.org/10.1016/0012-821X(95)00214-W

Malin, S. R. C., Hodder, B. M., and Barraclough, D. R. (1983). Geomagnetic secular variation: A jerk in 1970. *Scientific Contributions in Commemoration of Ebro Observatory's 75th Anniversary*., 239–256.

Olsen, N., and Mandea, M. (2007). Will the magnetic North Pole move to Siberia?. *Eos*, *Trans. AGU*, *88*(29), 293. https://doi.org/10.1029/2007eo290001

Olsen, N., and Mandea, M. (2008). Rapidly changing flows in the Earth's core. *Nat. Geosci.*, *1*(6), 390–394. https://doi.org/10.1038/ngeo203

Pinheiro, K., and Jackson, A. (2008). Can a 1-D mantle electrical conductivity model generate magnetic jerk differential time delays?. *Geophys. J. Int.*, *173*(3), 781–792. https://doi.org/10.1111/j.1365-246x.2008.03762.x

Pinheiro, K. J., Jackson, A., and Finlay, C. C. (2011). Measurements and uncertainties of the occurrence time of the 1969, 1978, 1991, and 1999 geomagnetic jerks. *Geochem., Geophys., Geosyst.*, *12*(10), Q10015. https://doi.org/10.1029/2011gc003706

Qamili, E., De Santis, A., Isac, A., Mandea, M., Duka, B., and Simonyan, A. (2013). Geomagnetic jerks as chaotic fluctuations of the Earth's magnetic field. *Geochem., Geophys., Geosyst.*, *14*(4), 839–850. https://doi.org/10.1029/2012GC004398

Torta, J. M., Pavón-Carrasco, F. J., Marsal, S., and Finlay, C. C. (2015). Evidence for a new geomagnetic jerk in 2014. *Geophys. Res. Lett.*, *42*(19), 7933–7940. https://doi.org/10.1002/2015GL065501

Verbanac, G., Korte, M., and Mandea, M. M. (2009). Four decades of European geomagnetic secular variation and acceleration. *Ann. Geophys.*, *52*(5), 487–503. https://doi.org/10.4401/ag-4605

Wardinski, I., and Holme, R. (2011). Signal from noise in geomagnetic field modelling: Denoising data for secular variation studies. *Geophys. J. Int.*, *185*(2), 653–662. https://doi.org/10.1111/j.1365-246x.2011.04988.x